

Fabrics in Polar Ice Sheets: Development and Prediction

RICHARD B. ALLEY

Fabrics in polar ice sheets provide a record of deformational history and control the viscosity of ice during further deformation; they affect geophysical sensing of ice sheets and provide an accessible analogue to fabric development during deformation of other geological and engineering materials. A new synthesis of experimental and theoretical results shows that c -axis fabrics are quantitatively related to cumulative strain and stress state in ice sheets for the full range of likely flow patterns. Basal shear, divergent flow, and parallel flow cause c axes to rotate toward the vertical axis, whereas convergent flow causes c axes to rotate toward a vertical plane transverse to flow.

THE VISCOSITY OF AN ICE CRYSTAL IS more than an order of magnitude less parallel to its basal plane than perpendicular to it (1, 2), and this anisotropy causes c axes in ice crystalline aggregates to rotate during deformation. Such c -axis fabrics record the deformational history of ice and affect the rate of further deformation. I combine computer simulations with recent observations to develop a unified hypothesis that predicts the distribution of different c -axis fabrics in polar ice sheets.

Ice grains that are constrained laterally by adjacent grains in a polycrystalline aggregate deform by basal glide coupled with c -axis rotation toward compressional axes and away from tensional axes (3). Diffusion, grain-boundary sliding, or dislocation climb or glide on prismatic planes (2) accommodate incompatible deformations between grains.

The longitudinal strain, ϵ_g , in a grain with its c axis at angle ϕ to the axis for uniaxial compression (4) or tension is proportional to the geometric factor (the Schmid factor, S) in the resolved shear stress across its basal plane such that (3)

$$S = \cos\phi\sin\phi$$

In uniaxial compression (4), strain of a grain with its c axis at angle ϕ causes rotation to angle ϕ_1 such that (3)

$$\sin\phi_1 = (1 + \epsilon_g)\sin\phi$$

For uniaxial tension (4), this becomes (5)

$$\cos\phi_1 = (1 + \epsilon_g)^{-1}\cos\phi$$

Pure shear (4) is the superposition of uniaxial compression and equal uniaxial tension

along orthogonal axes. These relations, plus the requirement that ϵ_g averaged over all grains in a polycrystalline aggregate equals the bulk strain (3, 5), allow numerical simulation of fabric development through c -axis rotation under a constant stress state (Fig. 1). The change in ϕ for an incremental bulk strain, $\Delta\epsilon$, is

$$\Delta\phi = \Delta\epsilon\sin^2\phi/\bar{S}$$

in uniaxial compression and

$$\Delta\phi = \Delta\epsilon\cos^2\phi/(\bar{S} + S\Delta\epsilon)$$

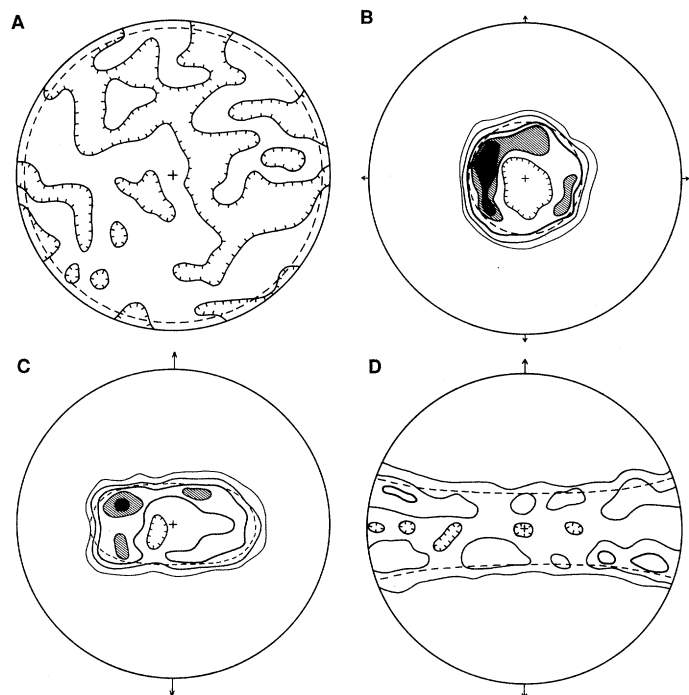
in uniaxial tension, for ϕ between 0° and 90° and where \bar{S} is the average of S over all

grains. For a given bulk strain, grains that have their c axes close to the compressional axis rotate less than grains that have c axes at higher angles. This difference in rotation rate causes development of small-circle girdles at intermediate strains (Fig. 1).

The parameter \bar{S} is the geometric softness of ice to uniaxial deformation (5); it varies with total strain (Fig. 2). Ice softens at small strains in uniaxial compression (Fig. 2A) because the median value of ϕ , $\bar{\phi}$, in a uniform distribution of ice crystals is 60° , and $\bar{\phi}$ initially decreases toward the position of maximum resolved shear stress at $\bar{\phi}$ equal to 45° . Ice hardens gradually at large strains as $\bar{\phi}$ becomes less than 45° (5, 6); strain in excess of 100% is required to halve \bar{S} (Fig. 2).

Simple shear, such as the basal shear in ice sheets, combines pure shear (Fig. 1C) with coplanar rigid-body rotation. It causes c axes to rotate toward ϕ equals 45° , where ϕ is measured from the compressive axis in the direction of rigid-body rotation. Thus c axes tend to cluster toward the vertical in ice-sheet basal shear. Ice in simple shear softens with increasing strain for all strains because the limiting position for rotation also is the position of maximum \bar{S} . In addition, in this limiting position the slip vectors are nearly parallel, so that the ice at high strains behaves somewhat like a monocrystal. In contrast, for the case of only normal stresses (7), basal planes become nearly parallel but the slip vectors have random azimuths, and the slip of any grain is constrained by neighbor-

Fig. 1. Simulated c -axis fabric diagrams on Schmidt nets. Two hundred points were generated and contoured (31) at 9, 7, 5, 3, and 1% area of the projection; (+) indicates the vertical ($\phi = 0$), and the dashed line marks the cone containing 90% of c axes. Hachures are toward decreasing density. Horizontal tensional axes are shown by arrows. (A) Randomly generated distribution; 90% cone is centered on the vertical; (B) to (D) show deformation of (A) to octahedral shear strain $\bar{\gamma}_0 = 1$ (32) under various stress states; (B) distribution after 50% vertical uniaxial compression (unit length to length 0.5); (C) distribution after pure shear deformation with 45% vertical compression and 85% longitudinal extension (unit length by unit length to lengths 0.55 by 1.85); (D) distribution after 100% longitudinal uniaxial extension (unit length to length 2); the dashed line marks the cone containing 10% (excluding 90%) of the c axes centered on the tensional axis.



Geophysical and Polar Research Center, University of Wisconsin, Madison, WI 53706.

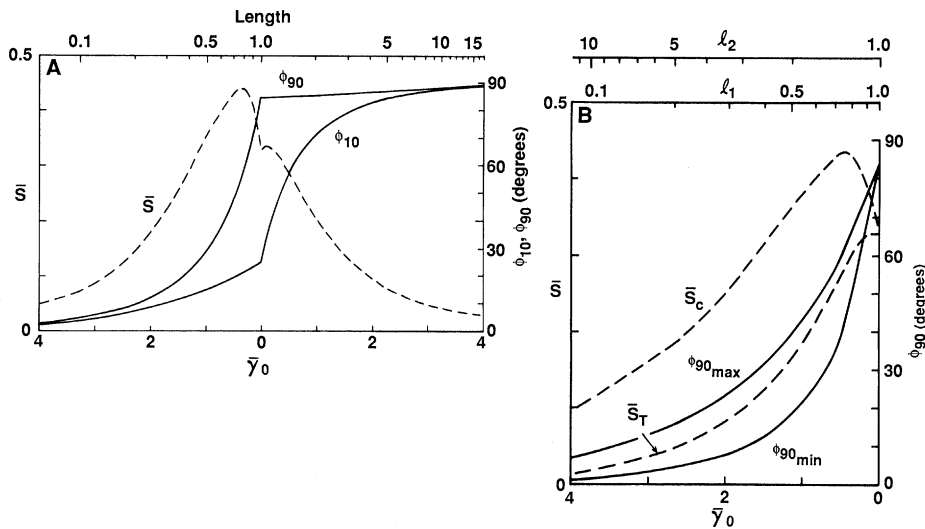


Fig. 2. Simulated evolution of geometric softness, $\bar{S} = \overline{\cos\phi\sin\phi}$, and cone half-angles, ϕ_x , for stress states in Fig. 1; (A) evolution in uniaxial tension and compression, plotted against the octahedral shear strain, $\bar{\gamma}_0$ (32), and the length along the unique stress axis for a sample that was initially a unit cube. ϕ_{10} and ϕ_{90} are the half-angles of the cones that are centered on the unique axis and contain 10% and 90% of the c axes, respectively; (B) evolution in pure shear, computed by superposing uniaxial compression and equal uniaxial tension on orthogonal axes. l_1 and l_2 are lengths along the compressional and tensional axes, respectively, for a sample that was initially a unit cube. \bar{S}_C and \bar{S}_T are softnesses to the compression and tension, respectively, and $\phi_{90_{\max}}$ and $\phi_{90_{\min}}$ are the maximum and minimum angles from the compressional axis to the surface that initially was the cone that was centered on the compression axis and contained 90% of the c axes.

ing grains. Ice in simple shear thus is softer than ice under only normal stresses for any given \bar{S} by approximately an order of magnitude (6).

Grain rotation will dominate fabric development until sufficient strain energy is stored to cause recrystallization, the nucleation and growth of new, strain-free grains (8). Recrystallization leads to development of a distinctive texture of large, interpenetrating grains (9) and of a distinctive fabric in which c axes and a axes cluster into multiple maxima (10). Because deformation does not cause a axes to cluster (1), crystallographic control of a -axis fabrics during recrystallization, possibly by twinning, is a likely mechanism (10). New grains nucleate with their basal planes near positions of maximum resolved shear stress and then rotate as described above until consumed by newer, less-strained grains (11, 12). A recrystallization fabric resembles the rotation fabric formed under the same stress orientation, but c axes in recrystallization fabrics generally form multiple maxima and do not occur near (within 5° to 10° of) the limiting position for c -axis rotation.

Recrystallization is favored by high temperature, large total strain, and high stress (13, 14). Recrystallization is more rapid under normal stresses than under simple shear because the incompatibility of deformation between adjacent grains and the hardening of ice with increasing strain under normal stresses cause large amounts of strain energy to be stored.

Observations of fabrics in ice sheets are readily interpreted by the use of this model. Cold ($\approx -10^\circ\text{C}$) regions of ice sheets that are dominated by normal stresses (typically the upper half of ice sheets, where longitudinal extension and vertical compression commonly occur) and with relatively low strain rates ($\approx 10^{-4}$ year $^{-1}$) should experience progressive rotation of c axes without significant recrystallization. At Dome C (15) and Byrd Station (9), Antarctica, and Camp Century (16) and Dye 3 (17, 18), Greenland, and other sites, c axes are observed to cluster about the vertical. These sites are characterized by divergent flow (transverse extension equals uniaxial vertical compression, Fig. 1B) or parallel flow (transversely neutral, pure shear, Fig. 1C) (19).

In cases of parallel flow, for example at Byrd Station and Dye 3, the cluster of c axes plotted on an equal-area net appears elliptical rather than circular, much like Fig. 1C (20). Local maxima within the overall cluster are observed in fabric diagrams from these sites, but these maxima have less than 5% of c axes per 1% area and may not be statistically significant (13). Development of these weak multiple maxima is accompanied by a cessation of increase in the average grain size (9, 18). It is possible that this cessation of grain growth marks the onset of slow dynamic recrystallization, and that continued growth among existing grains is balanced by nucleation of new grains at sites with high stored strain energy. Crystallographic control of the new nuclei thus might

explain the observed multiple maxima. The weakness of these multiple maxima and the continued tightening of c -axis fabrics with depth show that rotation is dominant over recrystallization in this region (21).

At Mizuho (5) and Vostok (6, 22) stations, Antarctica, c axes cluster about a vertical plane that is transverse to flow at Mizuho and suspected to be transverse at Vostok. Available data indicate that the flow leading to each site is characterized by lateral and vertical convergence of similar magnitude (uniaxial longitudinal extension, Fig. 1D) (23).

Thus, in the upper regions of ice sheets where normal stresses dominate and flow is longitudinally extensional and vertically compressional, transversely divergent flow causes symmetric rotation of c axes toward the vertical; transversely neutral flow (two-dimensional flow) causes rotation toward the vertical but also causes a transverse elongation of the distribution; and transversely convergent flow causes rotation toward a transverse vertical plane. Because the distribution of c axes is essentially uniform at 10-m depth in ice sheets (9), the tightness and shape of a c -axis distribution measured on an ice core taken from ice that has been deformed predominantly by grain rotation give a quantitative estimate of the cumulative strain, stress state, and softness of the sample (Fig. 2) (3, 5, 6).

Near the glacier bed, where basal shear stress is larger than the normal stress, a strong single-maximum fabric develops that has 90% of the c axes within about 30° of the vertical and with more than 25% of the c axes per 1% area within about 5° of vertical (9, 17, 18). This single-maximum fabric occurs in fine-grained ice that exhibits undulose extinction and kink banding (9) but no clustering of a axes (10). The tight clustering of c axes near the vertical rather than near 45° from the vertical, where recrystallization nuclei would form (11, 12), shows that rotation is dominant over recrystallization, even though strain rates can be as large as 10^{-1} year $^{-1}$ (24); lack of clustering of a axes also implies that rapid recrystallization does not occur in this region (10).

At greater depths in the ice sheets at Byrd Station (9) and Law Dome (25), Antarctica, c -axis fabrics change from single-maximum fabrics to small-circle girdle fabrics with multiple maxima that are centered about 25° to 30° from the vertical. Most (90%) of the c axes fall within about 45° to 50° of the vertical, and concentrations are less than 1% per 1% area within about 5° of vertical. Ice in this region is coarse grained, shows little undulose extinction or other optical evidence of lattice strain (9), and exhibits a -axis clustering (10). This fabric develops

through recrystallization, probably in response to the combined influence of high temperatures ($\geq -10^\circ\text{C}$) and high strain rates (13); fluctuations in magnitude or orientation of stresses also may help form this fabric (25). High strain rates and fluctuating stresses characterize the base of the Greenland ice sheet at Camp Century and Dye 3, but temperatures are less than -13°C and a single-maximum fabric is developed (16–18, 24, 26). Recrystallization under strong basal shear thus seems to require high temperatures. The importance of fluctuating stresses is still uncertain.

A multiple-maximum recrystallization fabric is developed on ice shelves (11, 27); c -axis concentrations are greater than 10% per 1% area at temperatures less than -20°C at shallow depth, and concentrations strengthen with increasing temperature and strain at greater depth (27). Ice shelves are dominated by normal stresses, and strain rates are greater than $\sim 10^{-3}$ year $^{-1}$. Comparison to inland regions shows that strain rates must be greater than $\sim 10^{-3}$ year $^{-1}$ to cause rapid recrystallization under normal stresses at temperatures less than $\sim -10^\circ\text{C}$, but that strain rates greater than $\sim 10^{-1}$ year $^{-1}$ and temperatures greater than $\sim -10^\circ\text{C}$ are necessary for recrystallization under simple shear.

The textures, temperatures, and strain rates in ice shelves with multiple-maximum fabrics are similar to those at the UpB camp on ice stream B, Antarctica (28, 29). This suggests that recrystallization also dominates at UpB. Strain at UpB is longitudinally extensional and vertically and transversely compressional (29); therefore, my model predicts that a fabric similar to that of Fig. 1D but with local concentrations arising from recrystallization should occur. Preliminary seismic results from ice stream B indicate that c axes do cluster near a transverse vertical plane (30), as predicted.

A complex strain history commonly leads to a complex fabric. Strains in excess of 100% may be required to remove evidence of a previous fabric by way of grain rotation; however, recrystallization will reduce the strain that is needed to generate a new fabric (2).

REFERENCES AND NOTES

1. P. V. Hobbs, *Ice Physics* (Clarendon, Oxford, 1974), pp. 274–280.
2. P. Duval *et al.*, *J. Phys. Chem.* **87**, 4066 (1983).
3. N. Azuma and A. Higashi, *Ann. Glaciol.* **6**, 130 (1985).
4. In an incompressible plastic such as ice, uniaxial compression has $\epsilon_2 = \epsilon_3 = -\epsilon_1/2$, where ϵ_i are the principal stress deviators, $\epsilon_1 < 0$ is compressive, and $\epsilon_3 > 0$ is extensional. Uniaxial tension has $\epsilon_1 = \epsilon_2 = -\epsilon_3/2$, and pure shear has $\epsilon_1 = -\epsilon_3$, $\epsilon_2 = 0$.
5. S. Fujita, M. Nakawo, S. Mae, *Proc. Natl. Inst. Polar Res. (Jpn)* No. 1 (1987), p. 122.
6. P. Pimienta, P. Duval, V. Ya. Lipenkov, *Int. Assoc. Hydrological Sci. Publ.* **170** (1987), pp. 57–66.

7. Stresses that do not cause rigid-body rotations are “normal” or “irrotational” stresses.
8. Growth selection, the growth of grains that are favorably oriented in the stress field at the expense of other grains, may be important in some cases but generally produces fabrics similar to those provided by recrystallization.
9. A. J. Gow and T. Williamson, *U.S. Army Corps Eng. Cold Reg. Res. Eng. Lab. Rep.* **76-35** (1976), pp. 1–25.
10. M. Matsuda and G. Wakahama, *J. Glaciol.* **21**, 607 (1978).
11. W. F. Budd, *Z. Gletscherk. Glazialgeol.* **8**, 65 (1972).
12. B. Kamb, in *Flow and Fracture of Rocks*, *Geophysical Monograph* **16**, N. C. Heard, I. Y. Borg, N. C. Carter, C. B. Raleigh, Eds. (American Geophysical Union, Washington, DC, 1972), pp. 211–241.
13. R. L. Hooke and P. J. Hudleston, *J. Glaciol.* **25**, 195 (1980).
14. R. W. Cahn, in *Physical Metallurgy*, R. W. Cahn and P. Haasen, Eds. (North-Holland, Amsterdam, ed. 3, 1983), part II, pp. 1595–1671.
15. D. D. Blankenship and C. R. Bentley, *Int. Assoc. Hydrological Sci. Publ.* **170** (1987), pp. 17–28.
16. S. L. Herron and C. C. Langway, Jr., *Ann. Glaciol.* **3**, 118 (1983).
17. K. Taylor, thesis, University of Wisconsin–Madison (1982).
18. S. L. Herron *et al.*, in *Greenland Ice Core: Geophysics, Geochemistry, and the Environment*, *Geophysical Monograph* **33**, C. C. Langway, H. Oeschger, W. Dansgaard, Eds. (American Geophysical Union, Washington, DC, 1985), pp. 23–31.
19. D. J. Drewry, Ed., *Antarctica: Glaciological and Geophysical Folio* (Scott Polar Research Institute, Cambridge, 1983); I. M. Whillans and S. J. Johnsen, *J. Glaciol.* **29**, 78 (1983); W. F. Budd and N. W. Young, in *The Climatic Record in Polar Ice Sheets*, G. de Q. Robin, Ed. (Cambridge Univ. Press, Cambridge, 1983), pp. 150–177; I. M. Whillans *et al.*, *Ann. Glaciol.* **5**, 185 (1984).
20. The statistical significance of this ellipticity is uncertain (13), and its orientation relative to the stress axes has not been measured directly because azimuthally oriented cores were not collected.
21. Alternatively, the stress state may limit grain-boundary motion to narrow zones between grains; therefore, grain growth stops because no grains are consumed by neighbors [P. Pimienta and P. Duval, *J. Phys.* **48**, Colloque C1, 243 (1987)]. If this happens, then recrystallization, which would decrease grain sizes, does not occur.
22. P. Pimienta, P. Duval, V. Ya. Lipenkov, A. N. Salamatin, *Ann. Glaciol.* **10**, 137 (1988).
23. R. Naruse and H. Shimizu, *Mem. Natl. Inst. Polar Res. (Jpn)*, *Spec. Issue* **7** (1978), p. 227. The flow just at Mizuho shows vertical extension because of local topography (Y. Abe, A. Yoshimura, R. Naruse, *ibid.*, p. 37), but flow lines and thickness patterns suggest approximately longitudinal uniaxial extension along most of the flow line leading to Mizuho; O. N. Vinogradov, *Trans. Soviet Antarct. Exped.* **60**, 100 (1972).
24. D. Dahl-Jensen and N. S. Gundestrup, *Int. Assoc. Hydrological Sci. Publ.* **170** (1987), pp. 31–43.
25. N. W. Young *et al.*, *Aust. Natl. Antarct. Res. Exped. Res. Notes* **28** (1985), pp. 18–24.
26. G. de Q. Robin, in *The Climatic Record in Polar Ice Sheets*, G. de Q. Robin, Ed. (Cambridge Univ. Press, Cambridge, 1983), pp. 94–97.
27. A. J. Gow, *U.S. Army Corps Eng. Cold Reg. Res. Eng. Lab. Rep.* **282** (1970), pp. 1–20.
28. R. B. Alley and C. R. Bentley, *Ann. Glaciol.*, in press.
29. I. M. Whillans, personal communication.
30. D. D. Blankenship and C. R. Bentley, *Ann. Glaciol.*, in press.
31. C. C. Langway, Jr., *U.S. Army Snow, Ice, Permafrost Res. Est. Tech. Rep.* **62** (1958), pp. 1–16.
32. The natural octahedral unit shear, $\bar{\gamma}_0$, is given by $\bar{\gamma}_0 = (2/3)[(\epsilon_1 - \epsilon_2)^2 + (\epsilon_2 - \epsilon_3)^2 + (\epsilon_3 - \epsilon_1)^2]^{1/2}$ where ϵ_i are the principal strains (13).
33. I thank C. R. Bentley, D. D. Blankenship, S. T. Rooney, and an anonymous reviewer for helpful suggestions and A. N. Mares and S. H. Smith for manuscript and figure preparation. Supported by the NSF Division of Polar Programs. This is contribution number 493 of the Geophysical and Polar Research Center, University of Wisconsin–Madison.

9 December 1987; accepted 24 February 1988

Superconducting and Magnetic Behavior in $\text{La}_{2-x}\text{Na}_x\text{CuO}_4$

M. A. SUBRAMANIAN, J. GOPALAKRISHNAN, C. C. TORARDI, T. R. ASKEW, R. B. FLIPPEN, A. W. SLEIGHT, J. J. LIN, S. J. POON

New phases of the type $\text{La}_{2-x}\text{A}_x^{1+}\text{CuO}_{4-y}$ have been prepared where A^{1+} is sodium or potassium. The sodium phases are superconducting for x values from 0.2 to 0.5 at temperatures up to about 40 K. In addition, there are unusual magnetic properties below about 10 K that may be indicative of spin glass behavior. Phases of the type $\text{La}_{2-x}\text{K}_x\text{CuO}_{4-y}$ could only be prepared with x values up to about 0.1, and these phases are not superconducting above 4.2 K.

FOLLOWING THE DISCOVERY OF high-temperature superconductivity in the La-Ba-Cu-O system by Bednorz and Müller (1), it has been shown that alkaline-earth metal substitution in La_2CuO_4 , $\text{La}_{2-x}\text{A}_x\text{CuO}_4$ where A is calcium, strontium, or barium, gives rise to superconductivity in this system in the 20 to 40 K range (2). One of us (3) has argued that superconductivity in this system is closely related to the strong electropositive character of A atoms that can stabilize Cu^{III} and render the Cu–O bonds more covalent.

This hypothesis is further strengthened by the observation that substitution of Pb^{II} and Cd^{II} in La_2CuO_4 does not give rise to superconductivity (4). Accordingly, we have studied the substitution of strongly electropositive alkali metal cations into La_2CuO_4 . Prior attempts (5) to substitute potassium in

M. A. Subramanian, J. Gopalakrishnan, C. C. Torardi, T. R. Askew, R. B. Flippen, A. W. Sleight, Central Research and Development Department, E. I. du Pont de Nemours and Company, Experimental Station, Wilmington, DE 19898.
J. J. Lin and S. J. Poon, Department of Physics, University of Virginia, Charlottesville, VA 22906.